

# PCCP

Accepted Manuscript



This is an *Accepted Manuscript*, which has been through the Royal Society of Chemistry peer review process and has been accepted for publication.

*Accepted Manuscripts* are published online shortly after acceptance, before technical editing, formatting and proof reading. Using this free service, authors can make their results available to the community, in citable form, before we publish the edited article. We will replace this *Accepted Manuscript* with the edited and formatted *Advance Article* as soon as it is available.

You can find more information about *Accepted Manuscripts* in the [Information for Authors](#).

Please note that technical editing may introduce minor changes to the text and/or graphics, which may alter content. The journal's standard [Terms & Conditions](#) and the [Ethical guidelines](#) still apply. In no event shall the Royal Society of Chemistry be held responsible for any errors or omissions in this *Accepted Manuscript* or any consequences arising from the use of any information it contains.



Journal name

ARTICLE

## Poly(ionic liquid)s as phase splitting promoters in aqueous biphasic systems†

Karen G. João,<sup>a‡</sup> Liliana C. Tomé,<sup>a‡</sup> Mehmet Isik,<sup>b</sup> David Mecerreyes,<sup>bc</sup> and Isabel M. Marrucho<sup>\*a</sup>

Received 00th January 20xx,  
Accepted 00th January 20xx

DOI: 10.1039/x0xx00000x

[www.rsc.org/](http://www.rsc.org/)

Aqueous biphasic systems (ABSs) provide a sustainable and efficient alternative to conventional liquid-liquid extraction techniques with volatile organic solvents, and can be used for extraction, recovery, and purification of diverse solutes. In this work, and for the first time, ABSs composed of poly(ionic liquid)s (PILs) and inorganic salts were measured at 25 °C and atmospheric pressure. New PILs having pyrrolidinium polycations combined with different counter-anions, namely acetate [Ac], trifluoroacetate [TFAc], hexanoate [Hex], adipate [Adi], and citrate [Cit] were synthesized, by a simple and environmentally-friendly procedure, and characterized. The effect of the PIL features, namely molecular weight and anion's character, and other experimental variables, such as temperature, on the phase splitting ability was researched. The aptitude of the studied ABS to be implemented as separation technologies was also evaluated through the use of a model biomolecule, tryptophan.

### Introduction

Poly(ionic liquid)s or polymeric ionic liquids (PILs) are a new class of polymeric materials that combine some of the unique properties of ionic liquids (ILs) and the intrinsic polymer features. The concept behind the definition of PILs is solely based on how they are generated by the (formal) polymerization of an IL monomer, in opposition to polyelectrolytes which are synthesized from solid salt monomers.<sup>1-4</sup> Since PILs are comprised of the corresponding IL specie in each monomer repeating unit connected through a polymeric backbone, some of the key properties of ILs such as ionic conductivity and tuneable solution properties are incorporated into the polymeric material.<sup>2,3</sup> Nevertheless, the physical properties of PILs and ILs are sometimes similar but not necessarily related to each other.<sup>4</sup>

The development of PILs has been following the initial trends of ILs, where counter-anions containing halides or fluorine atoms and polycations cations bearing imidazolium,<sup>5-10</sup> pyridinium,<sup>11</sup> piperidinium,<sup>12</sup> pyrrolidinium,<sup>12</sup> or ammonium moieties,<sup>11,13</sup> were the first to be synthesized by conventional free radical polymerization of IL monomers or via chemical modification of existing polymers. A few years ago, when the

first comprehensive reviews on PILs came out,<sup>1-3</sup> these polymers most prominent applications dealt with their conductivity and self assembly properties as ionic conductors in electrochemical devices,<sup>14-17</sup> dispersants and stabilizers,<sup>18-21</sup> carbon dioxide sorbents,<sup>22, 23</sup> sensitive materials,<sup>24, 25</sup> or precursors for carbon materials.<sup>26, 27</sup> Nowadays, PILs are being researched in terms of the tunability of their affinity properties and recent applications across diverse fields are being established, namely in gas separation and water purification membranes,<sup>28-31</sup> analytical chemistry,<sup>32</sup> smart materials,<sup>33</sup> energy,<sup>34</sup> and for bio-related applications.<sup>35</sup> This shift in interests is mainly due to the development of new PIL chemical structures, where the recent advances in the preparation of PILs by controlled/living radical polymerization techniques,<sup>4</sup> as well as the introduction of new types of cations and anions which are coming from the ionic liquid tool box,<sup>35-38</sup> are broadening the access to precisely designed IL species within a polymer matrix for each specific purpose.

In particular, and due to the high interest in polymers with lower critical solution temperature (LCST) type of phase transition, Ohno and co-workers developed PILs showing this phase behaviour, using their knowledge on the basic properties of the corresponding monomeric ILs.<sup>39</sup> These authors reported the synthesis of tetraalkylphosphonium styrenesulfonate and its anionic homopolymers, where they showed that hydrophobicity of the monomers and consequently the phase transition temperature of the homopolymer can be changed by varying the alkyl chain length of the phosphonium cations.<sup>33</sup> Conversely, Men *et al.* observed a similar behaviour for a cationic PIL bearing tributylbenzylphosphonium alkylsulfonate ion pair, where its phase transition behaviour in aqueous solution can be tuned by the alkyl chain length of the counter-anion.<sup>40</sup> In both cases,

<sup>a</sup> Instituto de Tecnologia Química e Biológica António Xavier, Universidade Nova de Lisboa, Av. República, 2780-157 Oeiras (Portugal), E-mail: [imarrucho@itqb.unl.pt](mailto:imarrucho@itqb.unl.pt).

<sup>b</sup> POLYMAT, University of the Basque Country UPV/EHU, Joxe Mari Korta Center, Avda. Tolosa 72, 20018 Donostia-San Sebastian (Spain).

<sup>c</sup> IKERBASQUE, Basque Foundation for Science, E-48011 Bilbao (Spain).

‡ Equally contributing authors

† Electronic Supplementary Information (ESI) available: NMR and FTIR spectra of the synthesized PILs, as well as the <sup>1</sup>H, <sup>19</sup>F and <sup>13</sup>C RMN spectra of the synthesized monomers. Experimental weight fraction data, phase diagrams, and experimental tie-lines of the ternary systems. See DOI: 10.1039/x0xx00000x

only one polymer (one chain length), whose aqueous solutions undergo LCST was obtained, indicating how rare this phenomenon is for strong polyelectrolytes as PILs.<sup>41</sup>

A simple way to tune the LCST phase behaviour of aqueous solutions of polyelectrolytes is through the addition of salting out salts, broadening the scope of “intelligent polymers” and smart materials. This technique can be of particular use for hydrophilic polymers, since new pathways for the synthesis of more sustainable PILs using natural and renewable resources are emerging.<sup>42, 43</sup> In particular, PILs with natural carboxylic acids as anion sources have been recently reported,<sup>44-46</sup> opening the perspective for the use of carboxylate counter-anions to prepare hydrophilic PILs, which have large potential in the development of more sustainable separation and purification systems.

The use of polymers in liquid-liquid separation and purification usually requires low polymer concentrations so that the viscosity of the phases in equilibrium is technologically acceptable. As mentioned before, a way to overcome this problem is by the simple addition of a salting out agent. This allowed the use of aqueous solutions of neutral or weakly charged polymers and salts at a fixed (low) temperature, where the two phases are promoted by inorganic salt concentration change. These polymer-salt aqueous systems have been widely exploited as a sustainable alternative to traditional liquid-liquid extraction techniques where volatile organic solvents are commonly used. The so-called aqueous biphasic systems (ABSs) are composed of two immiscible aqueous rich phases which occur when aqueous mixtures of two water soluble polymers, a single polymer and a salt or two salts are mixed together at appropriate concentrations and at a particular temperature. Although both solutes are water-soluble, they separate into two coexisting phases: one of the aqueous phases will be enriched in one of the solutes, while the other phase in the second polymer or salt. Polymer/polymer ABSs usually display two hydrophobic phases and the difference in polarities depends essentially on the amount of water present in each phase. On the other hand, polymer/salt ABSs present a hydrophobic phase constituted by the polymer and a hydrophilic (and more ionic) phase, typically formed by high charge-density salts. The possibility of creating ABSs through the addition of inorganic salts or polymers to aqueous solutions of ILs has been reported.<sup>47</sup> While Ohno and co-workers<sup>39</sup> showed that by manipulating the chain length in ILs, the hydrophobicity of the system can be tuned, Roger and co-workers<sup>48</sup> demonstrated the possibility of also tailoring their phase polarities by an adequate manipulation of the cation/anion design and their combinations. This aspect may become a major advantage of IL-based ABSs, given the limited polarity range presented by neutral or weakly charged polymer-based ABSs.

The recent ability to synthesize hydrophilic PILs combined with the use of inorganic salts to promote aqueous solutions liquid-liquid phase splitting enables the implementation of novel sustainable separation and purification systems, which to the best of our knowledge has never been explored. It is expected that due to the PIL inherent properties, these

systems should display all the above mentioned advantages of the IL-based systems, in particular the tailoring of the phase polarities. In this work, novel PILs having pyrrolidinium polycation backbone combined with different carboxylated counter-anions, namely acetate [Ac<sup>-</sup>], trifluoroacetate [TFAc<sup>-</sup>], hexanoate [Hex<sup>-</sup>], adipate [Adi<sup>-</sup>] and citrate [Cit<sup>-</sup>], were prepared in high yields by ring-closing free radical polymerization of the corresponding diallyldimethylammonium carboxylate monomers, and characterized. The counter-anions were chosen so provide insights on the role of the anion alkyl chain, by comparing poly([Pyr<sub>11</sub>][Ac]) with poly([Pyr<sub>11</sub>][Hex]), the introduction of substituent groups, by comparing poly([Pyr<sub>11</sub>][Hex]) with poly([Pyr<sub>11</sub>][Adi]) (adipate is a dicarboxylated counter-anion with six carbon atoms), and fluorination, by comparing poly([Pyr<sub>11</sub>][Ac]) with poly([Pyr<sub>11</sub>][TFAc]). Fig. 1 depicts the chemical structures of the PILs investigated. The effect of the polymer molecular weight in the phase equilibria was also explored by using poly([Pyr<sub>11</sub>][Cl]) with three different molecular weights. This is the first report where PILs are successfully used in the promotion of ABSs.

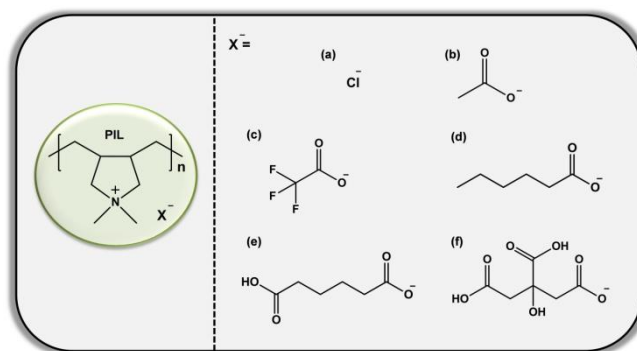


**Fig. 1** Chemical structures of poly([Pyr<sub>11</sub>][X]) (PILs) with the counter-anions: [X<sup>-</sup>] = (a) chloride (Cl<sup>-</sup>), (b) acetate ([Ac<sup>-</sup>]), (c) trifluoroacetate ([TFAc<sup>-</sup>]), (d) hexanoate ([Hex<sup>-</sup>]), (e) adipate ([Adi<sup>-</sup>]), and (f) citrate ([Cit<sup>-</sup>]).

## Results and discussion

### Synthesis and characterization of PILs

Generally, PILs can be synthesized by two strategies: (1) direct polymerization of IL monomers or (2) chemical modification of existing polymers.<sup>1-4</sup> From the synthetic point of view and depending on the target PIL, each strategy can comprise some advantages, as well as limitations, with respect to the molecular design. Concerning pyrrolidinium-based PILs, polymers with different chemical features were already synthesized by both synthetic strategies.<sup>49-56</sup> Although the second one is undoubtedly less complicated and very efficient since it solely consists in carrying out the anion exchange reaction directly into the commercially available poly(diallyldimethylammonium) chloride and the formed polymers precipitate in the aqueous media, this strategy is limited to prepare PILs having hydrophobic counter-anions.<sup>49-53</sup> Thus, when hydrophilic pyrrolidinium-based PILs are desired,

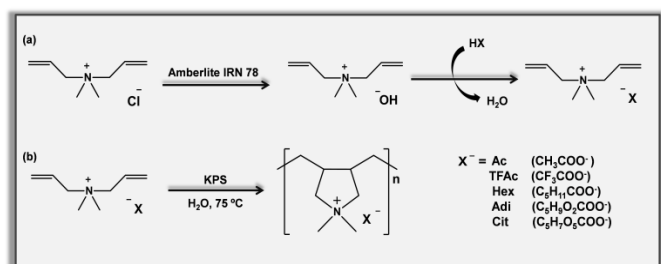


**Fig. 2** Synthetic pathways for (a) monomer preparation and their (b) polymerization.

the use of the first strategy is particularly more suitable.<sup>50</sup> Nevertheless, hydrophilic pyrrolidinium-based PILs having carboxylate counter-anions, namely acetate, trifluoroacetate and benzoate, were previously synthesized through a polymer anion exchange procedure using silver salts due to the low solubility of these salts in water which allows for their separation from the prepared polymers.<sup>54</sup> However, silver salts are very expensive and it is always difficult to completely remove the by-product silver halide from the resulting polymer aqueous solutions. Alternatively, in this work we successfully implemented an anion exchange procedure followed by neutralization reactions to prepare halide-free IL monomers with carboxylate anions as proposed by Ohno *et al.* for the synthesis of ILs.<sup>57, 58</sup> Actually, this is definitely a more economical and environmentally-friendly procedure that after polymerization affords highly pure pyrrolidinium-based PILs with carboxylate counter-anions.

Fig. 2 shows the synthetic pathways used to prepare the pyrrolidinium-based PILs containing carboxylate counter-anions. As mentioned before, diallyldimethylammonium-based monomers with the desired carboxylated anions were initially synthesized via a two-step anion exchange reaction (Fig. 2a). In a second step, the corresponding PILs were obtained by ring-closing free radical polymerization of the prepared IL monomers using water as solvent Fig. 2b.

The chemical nature of the synthesized PILs was confirmed by <sup>1</sup>H-NMR analysis and FTIR spectroscopy (spectra available in the Electronic Supplementary Information, ESI<sup>†</sup>). The success of the polymerization reaction can be easily seen from the <sup>1</sup>H-NMR spectra presented in Fig. S1 (ESI<sup>†</sup>). The signals associated to the vinylic protons between 5.5 and 6.0 ppm (see the <sup>1</sup>H-NMR spectra of the prepared IL monomers also provided in ESI<sup>†</sup>) disappeared after all the polymerization reactions, showing that complete conversion of the monomers was achieved. In addition, the characteristic chemical shifts arising from the pyrrolidinium polycation backbone can be clearly observed together with the proton signals associated to each corresponding carboxylated counter-anion. Similar information can also be obtained from the FTIR spectra of the synthesized

polymers (Fig. S2, ESI<sup>†</sup>). All spectra present absorption bands at around 1470 cm<sup>-1</sup> and bands between 2950 and 2850 cm<sup>-1</sup>, which are characteristic of -CH<sub>3</sub> bending vibrations originating from the pendant methyl units of the polycation backbone and -CH<sub>2</sub> stretching vibrations, respectively. The C=O stretching band was detected in all the spectra, between 1710 and 1650 cm<sup>-1</sup>, confirming the presence of carboxylated counter-anions in the polymer structure. A broad -OH stretching peak was also observed for all the pyrrolidinium-based PIL containing carboxylated counter-anions since these polymers are strongly hygroscopic.

Table 1 summarizes the molecular and thermal properties of the synthesized PILs. The molecular weights (*M<sub>w</sub>*) of the PILs were over 30 kDa. Although the pyrrolidinium-based PILs containing the [Ac]<sup>-</sup>, [Hex]<sup>-</sup>, and [Adi]<sup>-</sup> showed higher molecular weights (~ 50 kDa) than those having the [TFAc]<sup>-</sup> and [Cit]<sup>-</sup> counter-anions, further experiments need to be made to analyze the effect of the anion in the ring-closing free radical polymerization process.

The thermal stabilities of the prepared PILs were studied by TGA analysis. From Table 1, it can be seen that the poly([Pyr<sub>11</sub>][Cit]) has the lowest onset temperature (*T<sub>onset</sub>*), which is around 146 °C. After that, the PILs bearing the [Ac]<sup>-</sup> and the [Hex]<sup>-</sup> as counter-anions displayed *T<sub>onset</sub>* of roughly 175 °C and 180 °C, respectively. While for PILs containing the [TFAc]<sup>-</sup> or the [Adi]<sup>-</sup> as counter-anions, the *T<sub>onset</sub>* were above 200 °C. On the other hand, the decomposition temperature (*T<sub>dec</sub>*) trend of the PILs combining the different carboxylate counter-anions was found to be in the following order, from the lowest to the highest: [Hex]<sup>-</sup> < [Ac]<sup>-</sup> < [Cit]<sup>-</sup> < [Adi]<sup>-</sup> < [TFAc]<sup>-</sup>.

**Table 1.** Molecular and thermal properties of the prepared polymeric ionic liquids (PILs) containing different carboxylate counter-anions: average molecular weight (*M<sub>w</sub>*), onset (*T<sub>onset</sub>*), decomposition (*T<sub>dec</sub>*) and glass transition (*T<sub>g</sub>*) temperatures.

PILs	<i>M<sub>w</sub></i> (kDa) <sup>[a]</sup>	<i>T<sub>onset</sub></i> (°C) <sup>[b]</sup>	<i>T<sub>dec</sub></i> (°C) <sup>[c]</sup>	<i>T<sub>g</sub></i> (°C) <sup>[d]</sup>
Poly([Pyr <sub>11</sub> ][Ac])	52	180.5	208.0	-23.7
Poly([Pyr <sub>11</sub> ][TFAc])	41	206.0	248.6	-3.0
Poly([Pyr <sub>11</sub> ][Hex])	53	174.5	200.7	-13.0
Poly([Pyr <sub>11</sub> ][Adi])	50	218.5	244.3	-25.1
Poly([Pyr <sub>11</sub> ][Cit])	31	145.7	214.0	-10.4

[a] Average molecular weights measure by refractive index detector with respect to PS standards. [b] *T<sub>onset</sub>* defined as the temperature at which the first sharp decrease occurs during the heating. [c] *T<sub>dec</sub>* defined as the temperature at which 50% of weight is loss. [d] *T<sub>dec</sub>* defined as the temperature at the middle point of the glass transition region.

**Table 2.** Fitting parameters of Eq. (1) for the binodal experimental data, and respective standard deviations ( $\sigma$ ) and correlation coefficients ( $R^2$ ) for the PIL +  $K_3PO_4$  +  $H_2O$  ternary systems.

PILs	$T$ (°C)	$A \pm \sigma$	$B \pm \sigma$	$10^5 (C \pm \sigma)$	$R^2$
Poly([Pyr <sub>11</sub> ][Ac])	25	78 ± 1	-0.340 ± 0.005	7.2 ± 0.08	0.9999
Poly([Pyr <sub>11</sub> ][TFAc])	25	156 ± 6	-0.655 ± 0.013	9.6 ± 0.27	0.9998
Poly([Pyr <sub>11</sub> ][Cl]) <sup>[a]</sup>	25	92 ± 3	-0.428 ± 0.010	8.3 ± 0.22	0.9997
Poly([Pyr <sub>11</sub> ][Cl]) <sup>[a]</sup>	40	107 ± 3	-0.460 ± 0.010	6.6 ± 0.19	0.9997
Poly([Pyr <sub>11</sub> ][Cl]) <sup>[a]</sup>	50	132 ± 5	-0.513 ± 0.013	5.4 ± 0.21	0.9996
Poly([Pyr <sub>11</sub> ][Cl]) <sup>[b]</sup>	25	83 ± 2	-0.418 ± 0.008	8.3 ± 0.21	0.9997
Poly([Pyr <sub>11</sub> ][Cl]) <sup>[c]</sup>	25	84 ± 2	-0.411 ± 0.006	7.6 ± 0.14	0.9999
Poly([Pyr <sub>11</sub> ][Hex])	25	89 ± 1	-0.409 ± 0.005	12.4 ± 0.19	0.9998
Poly([Pyr <sub>11</sub> ][Adi])	25	12744 ± 4851	-1.597 ± 0.103	5.9 ± 0.94	0.9997
Poly([Pyr <sub>11</sub> ][Cit])	25	139 ± 7	-	12.3 ± 0.07	0.9998

[a] High  $M_w$  (400–500 kDa). [b] Medium  $M_w$  (200–350 kDa). [c] Low  $M_w$  (< 100 kDa).

The thermal properties of the prepared PILs were further studied by DSC. All the polymers were found to be amorphous having relatively low glass transition temperatures ( $T_g$ ), which were below 0 °C (Table 1). The poly([Pyr<sub>11</sub>][Adi]) and poly([Pyr<sub>11</sub>][Ac]) have the lowest  $T_g$ , around -25 °C and -23 °C, respectively, while the poly([Pyr<sub>11</sub>][TFAc]) presents the highest  $T_g$  (-3 °C). For pyrrolidinium-based PILs having the [Hex]<sup>-</sup> and [Cit]<sup>-</sup> as counter-anions, glass transition temperatures of -13 °C and -10 °C, were respectively obtained.

### Phase diagrams and tie-lines

As mentioned before, the aim of the present work is to evaluate the ability of the prepared PILs to induce the formation of ABS in aqueous solutions of  $K_3PO_4$ . Binodal curves of  $K_3PO_4$  +  $H_2O$  + PILs-based ternary systems were determined through the cloud point titration method at 25 °C and atmospheric pressure. The binodal

curves are presented in molality units to avoid differences that can result from the influence of the PIL molecular weight ( $M_w$ ). For each system, the molality of the polymer was calculated using their  $M_w$  estimated in this work. The experimental weight fraction data of the ternary systems are provided in Tables S1-S2 (ESI<sup>+</sup>).

Table 2 presents the parameters obtained by regression of the experimental binodal curves data (in weight fraction) for the studied systems using Eq. (1). Good correlation coefficients were obtained indicating that Eq. (1) provides a good description of the experimental data.

The tie-lines ( $TL$ ) and tie-line lengths ( $TLL$ ) were determined through the application of Eq. (2-6) for all the systems studied. In the case of poly([Pyr<sub>11</sub>][TFAc]) and poly([Pyr<sub>11</sub>][Cl]) it was not possible to determine the  $TL$ s accurately, due to the high viscosity of PIL-rich phase. The initial mixture composition and phases in equilibrium, as well as the respective  $TLL$  are summarized in Table 3.

**Table 3.** Weight percentage (wt%) of PIL ( $w_{PIL}$ ) and  $K_3PO_4$  ( $w_{K_3PO_4}$ ) in the initial mixture ( $M$ ), top phase ( $T$ ) and bottom phase ( $B$ ), and respective values of tie-line lengths ( $TLL$ ), at 25°C.

PILs	Weight percentage (wt%)						$TLL$
	$w_{PIL,M}$	$w_{K_3PO_4,M}$	$w_{PIL,T}$	$w_{K_3PO_4,T}$	$w_{PIL,B}$	$w_{K_3PO_4,B}$	
Poly([Pyr <sub>11</sub> ][Ac])	9.757	25.021	37.299	4.616	1.252	31.323	44.863
Poly([Pyr <sub>11</sub> ][Hex])	9.857	24.986	53.927	1.517	0.329	30.060	60.725
	20.329	24.767	59.862	0.955	0.014	37.004	69.866
Poly([Pyr <sub>11</sub> ][Adi])	9.945	25.210	60.175	10.928	0.789	27.814	61.739
	7.645	20.312	26.856	14.106	4.527	21.319	23.465
	8.481	20.264	29.777	13.690	4.248	21.571	26.718
Poly([Pyr <sub>11</sub> ][Cit])	4.944	32.763	56.285	19.398	1.023	33.785	57.104
	4.913	33.441	70.348	17.643	0.911	34.407	71.432
	4.115	31.923	45.068	20.876	1.185	32.714	45.452
	4.022	30.762	29.316	23.263	2.584	31.192	27.883

The results obtained for the *T*Ls of the systems composed of PIL +  $K_3PO_4$  +  $H_2O$  are shown in Fig. S14 (ESI<sup>†</sup>).

### Polymer's properties effect

Fig. 3 presents a comparison between the binodal curves for all the measured systems containing PILs with the objective of understanding the influence of the PILs' properties, in particular the polymer's molecular weight and the counter-anion's character, on ABS formation. The closer to the axes origin the binodal curve is, the lower is the PIL concentration required for ABS formation and consequently the stronger is the phase-forming ability of the PIL. The ability of the studied PILs to promote a biphasic system with  $K_3PO_4$  follows the trend of the counter-anions:  $Cl^- > [TFAc]^- > [Hex]^- > [Ac]^- > [Adi]^- > [Cit]^-$ .

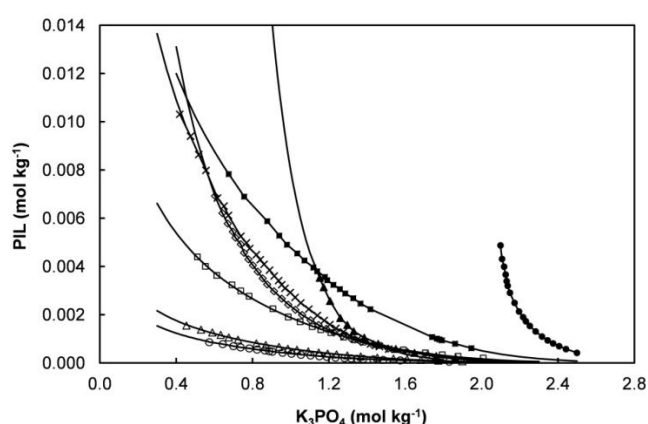


**Fig. 3** Phase diagrams of PIL +  $K_3PO_4$  +  $H_2O$  at 25 °C: Poly([Pyr<sub>11</sub>][Ac]) (■), Poly([Pyr<sub>11</sub>][TFAc]) (◇), Poly([Pyr<sub>11</sub>][Cl]) high  $M_w$  (400–500 kDa) (○), Poly([Pyr<sub>11</sub>][Cl]) medium  $M_w$  (200–350 kDa) (Δ), Poly([Pyr<sub>11</sub>][Cl]) low  $M_w$  (< 100 kDa) (□), Poly([Pyr<sub>11</sub>][Hex]) (×), Poly([Pyr<sub>11</sub>][Adi]) (▲), Poly([Pyr<sub>11</sub>][Cit]) (●). The lines correspond to the respective correlations derived from Eq. (1).

When working with ILs, the mechanism behind the phase formation of IL + inorganic salt (IS) ABS is the competition between the IL and the IS for the water molecules, which is won by the latter since ISs are more able to form hydration complexes. Therefore, the salting order of the ILs in IS aqueous solution follows the IL's hydrophobicity: the more hydrophobic the IL is, the easier it is to promote phase splitting and thus a larger biphasic region is obtained. In the case of PILs containing systems, another factor comes into discussion: the PIL molecular weight. In order to address this issue, poly([Pyr<sub>11</sub>][Cl]) with three different molecular weights, namely high  $M_w$  (400–500 kDa), medium  $M_w$  (200–350 kDa), and low  $M_w$  (< 100 kDa), were used. It can be observed in Fig. 3 that the higher the PIL's  $M_w$  is, the larger are the biphasic regions obtained, expressing more difficulty to accommodate bigger PIL chains, which have higher hydrophobic character, in water. The same effect was observed in other ABS systems containing non charged polymers, such as polymer + ISs,<sup>59</sup> and PEG or PPG + ILs.<sup>60–63</sup> It should be also

mentioned that even the poly([Pyr<sub>11</sub>][Cl]) with low  $M_w$  (< 100 kDa) is considerably larger than the other synthesized PILs having different carboxylated counter-anions ( $M_w$  between 31 and 53 kDa). Consequently, despite the high hydrophilicity of the chloride anion, the PIL phase behaviour is primarily determined by its  $M_w$ .

Since the other five studied PILs exhibit similar  $M_w$  (Table 1), it is possible to discuss now the probable mechanism in terms of the chemical features of the PIL's counter-anion only. For example, the effect of the counter-anion chain length can be evaluated by comparing the results for poly([Pyr<sub>11</sub>][Ac]) and poly([Pyr<sub>11</sub>][Hex]). In Fig. 3, it can be seen that the longer the alkyl chain length of the counter-anion is, larger immiscibility region is obtained, in agreement with the behaviour previously reported by us for ILs-based ABS.<sup>64</sup> On the other hand, when the alkyl chain length of the counter-anion is maintained but an extra carboxylate group is added, as in the case of poly([Pyr<sub>11</sub>][Hex]) and poly([Pyr<sub>11</sub>][Adi]), whose counter-anion's are derived from monoacid and diacid with six carbon atoms respectively, a decrease in the biphasic region was observed. This behaviour is in agreement with the increase of the counter-anion's hydrophilicity due to the introduction of an extra carboxylate group. In a similar manner, the poly([Pyr<sub>11</sub>][Cit]), whose counter-anion is derived from the citric acid, a triacid with six carbon atoms and an extra hydroxyl group, is the most hydrophilic PIL studied in this work as it can be clearly seen by the displacement of its binodal curve for higher salt concentrations. Regarding the introduction of fluorine atoms in the counter-anion, it can be concluded by comparing the results for poly([Pyr<sub>11</sub>][Ac]) and poly([Pyr<sub>11</sub>][TFAc]), that the presence of the trifluoromethane group in the counter-anion makes the respective PIL more hydrophobic than poly([Pyr<sub>11</sub>][Ac]) and also than all the other PILs with similar molecular weight.

Overall, it can be concluded that the phase-forming ability of the pyrrolidinium-based PILs with carboxylated counter-anions seems to be determined by the anion's hydrophobicity, or in other words, by their hydration capacity, following the results obtained for ILs and  $K_3PO_4$ .<sup>65–67</sup> Furthermore, the importance of the PILs  $M_w$  on its phase splitting ability can be here confirmed, the increase of the PILs  $M_w$  greatly increases its aptitude to phase splitting. This parameter can thus be used to tune the PILs hydrophilicity and produce new aqueous biphasic systems.

Additionally, Fig. 4 presents a comparison between the phase diagrams studied in this work with those of PEGs +  $K_3PO_4$  available in literature.<sup>68,69</sup> Only data for PEGs with  $M_w$  up to 8000 were found. The ability of PEGs to promote a biphasic system in aqueous solutions of  $K_3PO_4$  follows the trend:  $Cl^- > [TFAc]^- > [Hex]^- > PEG 8000 > [Ac]^- > PEG 6000 > PEG 3400 > PEG 4000 > PEG 2000 > [Adi]^- > PEG 1000 > [Cit]^-$ . Consequently, it can be observed that the phase boundaries for PEG containing systems lay in the same region as those of PILs containing systems studied in this work, although PILs have a much larger  $M_w$ . It should be kept in mind that PEGs are non-charged polymers with a different phase splitting mechanism in inorganic salt aqueous solutions than PILs. Nevertheless, the chemical features of the PIL's counter-anion has a great influence on the hydrophilicity of the polymer, making possible that PILs with much higher  $M_w$  be as hydrophilic as the low  $M_w$  PEGs.

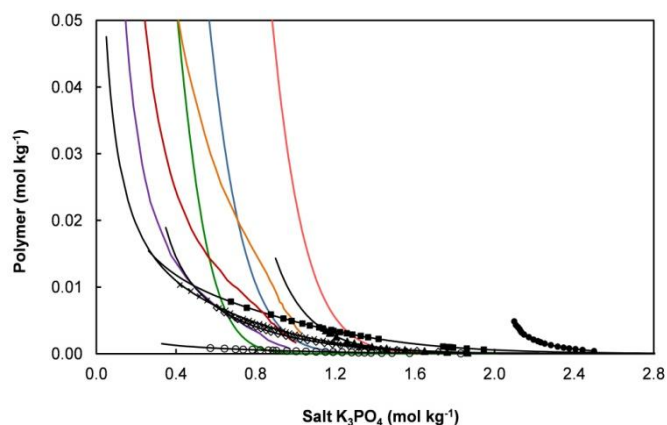


**Fig. 4** Phase diagrams of Polymer +  $K_3PO_4$  +  $H_2O$ : PEG 1000 (pink line), PEG 2000 (blue line), PEG 3400 (green line), PEG 4000 (orange line), PEG 6000 (red line), PEG 8000 (purple line), Poly([Pyr<sub>11</sub>][Ac]) (■), Poly([Pyr<sub>11</sub>][TFAc]) (◇), Poly([Pyr<sub>11</sub>Cl] high  $M_w$  (400–500 kDa) (○), Poly([Pyr<sub>11</sub>][Hex]) (×), Poly([Pyr<sub>11</sub>][Adi]) (▲), Poly([Pyr<sub>11</sub>][Cit]) (●). The black lines correspond to the respective correlations derived from Eq. (1).

### Temperature effect

In order to study the effect of temperature, phase equilibria measurements of the system poly([Pyr<sub>11</sub>]Cl) +  $K_3PO_4$  +  $H_2O$  were further performed at 40 and 50 °C. Fig. 5 shows that the phase diagrams display smaller immiscibility region as the temperature increases, indicating that higher temperatures require higher concentrations of salt and PIL for phase separation. This behaviour is in close agreement to what has been observed in ABS composed of ILs + inorganic salts, ILs + amino acids, ILs + carbohydrates, ILs + PEG, and polymer + polymer.<sup>47, 63, 70, 71</sup> However, in typical PEG + IS<sup>72-74</sup> and PVP + IS<sup>75</sup> ABS, an increase in temperature leads to a larger immiscibility region. Therefore, the temperature dependence of binodal curves for PIL + IS systems resembles that of IL + IS systems, revealing that some properties of these PILs are closer to ILs than that of conventional neutral polymers such as PEG and PVP. This can be explained by the fact that PILs comprise the

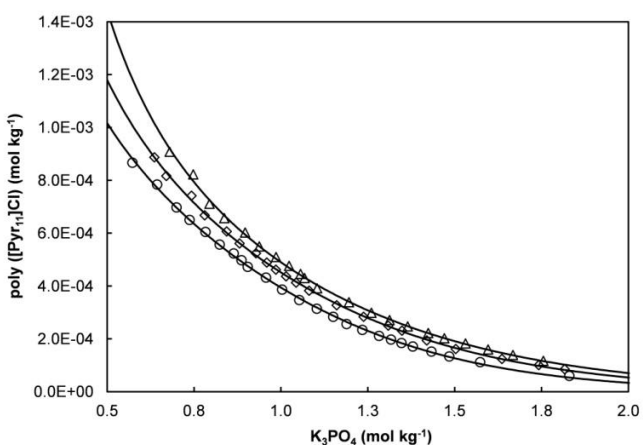


**Fig. 5** Phase diagrams for the poly([Pyr<sub>11</sub>]Cl) +  $K_3PO_4$  +  $H_2O$  ABS at: 25 °C (○), 40 °C (◇) and 50 °C (Δ). The lines correspond to the respective correlations derived from Eq. (1).

corresponding IL monomer repeating unit through the polymeric backbone, which in turn contributes to the incorporation of some of the unique properties of ILs into the polymeric material. This different nature is traduced in different phase splitting mechanisms since in IL + inorganic salt both enthalpic and entropic effects are at the origin of the phase clouding while in polymer + ISs the entropic effects dominate.

### pH, density and viscosity effect

The physicochemical properties of the two phases in equilibrium in the studied ABS, namely pH, density and viscosity are key features when the intent is to use these systems in extractive approaches for biomolecule's separation applications. Therefore, and in order to better evaluate the potential of ABS systems herein proposed, pH values, densities and viscosities of the coexisting phases were measured for the following ternary mixture compositions: 10 wt% of Poly([Pyr<sub>11</sub>][Ac]) or Poly([Pyr<sub>11</sub>][Hex]) + 25 wt% of  $K_3PO_4$ , 8 wt% Poly([Pyr<sub>11</sub>][Adi]) + 20 wt%  $K_3PO_4$  and 4 wt% of Poly([Pyr<sub>11</sub>][Cit]) + 20 wt %  $K_3PO_4$ . The results are presented in Table 4. These mixture compositions were chosen to be used to evaluate the extraction capacity of these systems of tryptophan.

**Table 4.** pH values, viscosity,  $\eta$  (mPa s), and density,  $\rho$  ( $g\ cm^{-3}$ ), of the coexisting phases in ABS composed of PILs +  $K_3PO_4$  +  $H_2O$  at 25 °C.

PILs	PIL-rich phase			$K_3PO_4$ -rich phase		
	pH	$\eta$	$\rho$	pH	$\eta$	$\rho$
Poly([Pyr <sub>11</sub> ][Ac])	12.37	795.857	1.105	12.79	4.541	1.334
Poly([Pyr <sub>11</sub> ][Hex])	8.73	390.897	1.068	12.83	3.163	1.318
Poly([Pyr <sub>11</sub> ][Adi])	7.54	16.266	1.180	12.67	2.763	1.219
Poly([Pyr <sub>11</sub> ][Cit])	6.59	32.307	1.292	12.72	4.151	1.336

From Table 4, it can be observed that inorganic salt rich phase is alkaline for all systems due to the presence of the basic  $PO_4^{3-}$  anion. The pH of PIL-rich phase is more diverse, ranging from 12.83 to 6.59, depending on the PIL used in the ABS.

The density of the  $K_3PO_4$ -rich phase is always higher than that of the PIL-rich phase for all the systems. However, for Poly([Pyr<sub>11</sub>][Cit])- and Poly([Pyr<sub>11</sub>][Adi])-based ABS similar density in both phases were obtained, indicating that for these systems phase separation is slower, which can be problematic for large-scale applications.

Viscosity is another property that is critical for any separation system. Table 4 shows that the viscosity of both phases are quite different, especially for the systems containing poly([Pyr<sub>11</sub>][Ac]) and poly([Pyr<sub>11</sub>][Hex]), where high viscosities for the PIL-rich phase were obtained. At 25 °C and for the compositions mentioned above, the viscosity of the PIL-rich phase decreases in the following order: poly([Pyr<sub>11</sub>][Ac]) (795.857 mPa s) > poly([Pyr<sub>11</sub>][Hex]) (390.897 mPa s) > poly([Pyr<sub>11</sub>][Cit]) (32.307 mPa s) > poly([Pyr<sub>11</sub>][Adi]) (16.266 mPa s). Nevertheless, note that the compositions of the PILs used in the Poly([Pyr<sub>11</sub>][Adi])- and poly([Pyr<sub>11</sub>][Cit])-based ABS are different from those used for the poly([Pyr<sub>11</sub>][Ac]) and poly([Pyr<sub>11</sub>][Hex]) systems. Therefore, the lower amount of poly([Pyr<sub>11</sub>][Adi]) and

poly([Pyr<sub>11</sub>][Cit]) used in these systems are responsible for the lower viscosities of these PIL-rich phases.

### Partitioning of L-tryptophan

In order to evaluate the performance of the proposed systems for extraction purposes, L-tryptophan (C<sub>11</sub>H<sub>12</sub>N<sub>2</sub>O<sub>2</sub>) was used as a model biomolecule and its partitioning behaviour between the coexisting phases of ABS formed by the studied PILs + K<sub>3</sub>PO<sub>4</sub> + H<sub>2</sub>O systems evaluated. This amino acid has an indole group in its chemical structure, that confers L-tryptophan hydrophobic characteristics.<sup>76</sup> Since the addition of L-tryptophan in small concentrations (0.80 g dm<sup>-3</sup>) has no significant influence on the *TLs* and *TLLs*,<sup>66, 67</sup> the systems prepared for the extraction of L-tryptophan using PILs + K<sub>3</sub>PO<sub>4</sub> + H<sub>2</sub>O were used to determine the *TLs*, *TLLs* and simultaneously the partition coefficients (*K*<sub>Trp</sub>).

There are several factors, such as hydrophobic and/or electrostatic interactions, nature and concentrations of PILs and inorganic salts, water solubility, pH and temperature, and nature of the biomolecules, that need to be taken into account when discussing their partition in ABS.<sup>76</sup> The partition coefficients (*K*<sub>Trp</sub>) and the extraction efficiencies (%EE) of L-tryptophan, as well as the respective ABS's composition at 25 °C, are reported in Table 5. For both poly([Pyr<sub>11</sub>][Ac]) and poly([Pyr<sub>11</sub>][Hex]) containing systems, initial mixture compositions of approximately 10 wt% of PIL and 25 wt% of K<sub>3</sub>PO<sub>4</sub> were used. However, for systems comprising poly([Pyr<sub>11</sub>][Adi]) and poly([Pyr<sub>11</sub>][Cit]), these concentrations were outside of the respective biphasic region and therefore different initial mixture compositions were used: 8 wt% of poly([Pyr<sub>11</sub>][Adi]) and 20 wt% of K<sub>3</sub>PO<sub>4</sub>, and 4 wt% of poly([Pyr<sub>11</sub>][Cit]) and 20 wt% of K<sub>3</sub>PO<sub>4</sub>.

The extraction efficiencies of L-tryptophan range between 47 % and 99%, showing that Poly([Pyr<sub>11</sub>][Hex])- and Poly([Pyr<sub>11</sub>][Ac])-based ABSs are more effective in the extraction of this biomolecule.

**Table 5.** Partition coefficients (*K*<sub>Trp</sub>) and extraction efficiencies (%EE) of L-tryptophan in ABS composed of PILs + K<sub>3</sub>PO<sub>4</sub> + H<sub>2</sub>O at 25 °C.

PILs	Weight fraction percentage		<i>K</i> <sub>Trp</sub>	%EE
	PIL	K <sub>3</sub> PO <sub>4</sub>		
Poly([Pyr <sub>11</sub> ][Ac])	9.757	25.021	126	97.6
Poly([Pyr <sub>11</sub> ][Hex])	9.857	24.986	453	99.0
Poly([Pyr <sub>11</sub> ][Adi])	7.645	20.312	5.41	47.4
Poly([Pyr <sub>11</sub> ][Cit])	4.022	30.762	20.0	53.7

The obtained partitioning coefficients of L-tryptophan range between 5.41 and 453, following the order: poly([Pyr<sub>11</sub>][Adi]) < poly([Pyr<sub>11</sub>][Cit]) < poly([Pyr<sub>11</sub>][Ac]) < poly([Pyr<sub>11</sub>][Hex]). The results indicate the preferential partitioning of L-tryptophan for the PIL-rich phase, since the *K*<sub>Trp</sub> is much larger than 1 for all the studied systems (Table 5). According to the results reported in the literature for the extraction of L-tryptophan with ABS composed of imidazolium-based ILs and K<sub>3</sub>PO<sub>4</sub>, L-tryptophan partitions preferentially for IL-rich phases composed of halogenated anions

such as Cl<sup>-</sup> or Br<sup>-</sup>, or the most hydrophobic anions.<sup>67</sup> Thus, the results obtained in the present work are in agreement with the literature, since L-tryptophan prefers PIL-rich phases composed by most hydrophobic anions.

What is more, the partition coefficients for L-tryptophan (Table 5) are substantially higher than those observed for conventional ABS composed of polymer + polysaccharide ABS (*K*<sub>Trp</sub> ≈ 1),<sup>77</sup> and polymer + ISs (*K*<sub>Trp</sub> 1–7).<sup>78</sup> Comparing the *K*<sub>Trp</sub> for the PILs-based ABS obtained in this work to those existent in the literature for alkyl-3-methylimidazolium-based ILs and K<sub>3</sub>PO<sub>4</sub> (*K*<sub>Trp</sub> 5–96),<sup>66, 67</sup> it is possible to conclude about the high performance of the PIL-based systems for the efficient extraction of this model biomolecule.

## Experimental

### Materials

Poly(diallyldimethylammonium) chloride solutions with different molecular weights (*M*<sub>w</sub>), namely high *M*<sub>w</sub> (average 400–500 kDa, 20 wt% in water), medium *M*<sub>w</sub> (average 200–350 kDa, 20 wt% in water), and low *M*<sub>w</sub> (average < 100 kDa, 35 wt% in water), SUPELCO Amberlite IRN-78, diallyldimethylammonium chloride solution (65 wt% in water), acetic acid (≥ 99%), trifluoroacetic acid (≥ 99%), hexanoic acid (≥ 99.5%), adipic acid (≥ 99%), citric acid (≥ 99.5%), diethyl ether (99.8%), potassium persulfate (KPS, ≥ 99%), potassium phosphate tribasic (K<sub>3</sub>PO<sub>4</sub>, ≥ 98%), and L-tryptophan (≥ 98 %) were supplied by Sigma-Aldrich and used as received. The water used in all the experiments was double distilled, passed through a reverse osmosis system and then treated with a Milli-Q plus 185 water purification equipment.

### Synthesis of monomers

Different IL type monomers based on the diallyldimethylammonium cation and carboxylated anions, namely acetate ([Ac]), trifluoroacetate ([TFAc]), hexanoate ([Hex]), adipate ([Adi]) and citrate ([Cit]), were synthesized via a two-step anion exchange reaction as shown in Fig. 2a. First, an aqueous solution of diallyldimethylammonium hydroxide was prepared by passing an aqueous solution of the commercially available diallyldimethylammonium chloride through a column filled with anion exchange resin (SUPELCO Amberlite IRN-78) in the hydroxide form. Subsequently, the prepared basic monomer solution was neutralized by slowly dropwise addition of a slight excess of the corresponding carboxylic acid, with cooling. The mixtures were stirred at ambient temperature and pressure for 12 h. Excess of water was then removed by rotary evaporation under reduced pressure. The resulting products were washed with diethyl ether in order to remove unreacted acid. After solvent removal by rotary evaporation, the obtained monomers (yields higher than 90%) were dried under vacuum (10<sup>-3</sup> kPa) at ≈ 45 °C for at least 4 days immediately prior to their polymerization. The chemical structures of the prepared diallyldimethylammonium carboxylate monomers were confirmed by NMR analysis (spectra available in ESI<sup>†</sup>).

### Synthesis of polymers

Ring-closing free radical polymerization in water was used to polymerize the prepared monomers Fig. 2b. In a typical experiment,

8 g of diallyldimethylammonium carboxylate monomer and 2 mL of water were mixed in a round bottom flask by stirring and purged with dry nitrogen for 30 min before the sealed flask was immersed in an oil bath at 75 °C. Then, an aqueous solution of initiator (0.24 g of KPS and 2.4 mL of water), previously prepared and bubbled with nitrogen, was gradually dropwise added to the monomer solution with vigorous stirring throughout 48 h of reaction in order to obtain total monomer conversion. The solid content of the polymerization reactions was 65 wt%, in which the amount of KPS initiator was 3 wt% with respect to the monomer content used. After polymerization of the different monomers, the resulting polymer solutions were dried in a vacuum oven until constant weights were attained. The obtained solid poly([Pyr<sub>11</sub>][Ac]), poly([Pyr<sub>11</sub>][TFAC]), poly([Pyr<sub>11</sub>][Hex]), poly([Pyr<sub>11</sub>][Adi]), and poly([Pyr<sub>11</sub>][Cit]) were then characterized and used without further purification.

### Polymer characterization

The pyrrolidinium-based PILs with carboxylate counter-anions synthesized in this work were characterized by Nuclear Magnetic Resonance (<sup>1</sup>H-NMR), Attenuated Total Reflection-Fourier Transform Infrared spectroscopy (ATR-FTIR), thermogravimetric analysis (TGA), differential scanning calorimetry (DSC), and gel permeation chromatography-size exclusion chromatography (GPC-SEC).

NMR spectra were recorded with a Bruker AC-500 spectrometer. The samples were dissolved in deuterium oxide, and the solutions were measured with tetramethylsilane as an internal reference.

Spectroscopic characterization of the polymers was obtained on a Bruker ALPHA ATR-FTIR spectrometer. All spectra were collected using 32 scans with a resolution of 2 cm<sup>-1</sup> from 650 to 4000 cm<sup>-1</sup>.

The thermal stabilities and decomposition temperatures of the prepared polymers were measured using a thermal gravimetric analyser (TGA Q500, TA Instrument). The samples were placed inside platinum pans and heated up to 800 °C, at a constant rate of 10 °C min<sup>-1</sup>, under a nitrogen atmosphere. The onset (*T*<sub>onset</sub>) and the decomposition (*T*<sub>dec</sub>) temperatures were determined, as the temperatures at which the baseline slope changes during the heating, and at which 50 % of weight loss was observed, respectively.

DSC experiments were performed on a TA Instrument Q2000. Samples (ca. 5 to 10 mg) were crimped in non-recyclable aluminium hermetic pans and analysed under nitrogen atmosphere by heating and cooling cycles at a rate of 10 °C min<sup>-1</sup>. First, the samples were heated to 150 °C and kept isothermal for 5 min to erase the thermal history of the samples. Then, they were cooled down to -70 °C and kept isothermal for 5 min. Second run heating cycles were conducted and analyzed. The glass transition (*T*<sub>g</sub>) temperatures were determined as the temperature at the midpoint of the glass transition region.

GPC-SEC system (Agilent PL-GPC 50) was used to estimate the molecular weight (*M*<sub>w</sub>) of the polymers using DMF containing 10 mM of LiBr as the eluent, at 50 °C and a flow rate of 1 mL min<sup>-1</sup>. Shodex mixed-bed KD-806M DMF GPC column was used. Molecular weights were determined with respect to narrow molecular weight Polystyrene standards.

### Phase diagrams and tie-lines determination

The phase diagrams were measured in a glass vessel and determined by the cloud point titration method at 25 °C and atmospheric pressure, as previously described.<sup>64-66, 79</sup> The vessel was provided with an external jacket in which water circulated at the given temperature (± 0.01 °C) using a Lauda E200 water thermostat and a Pt 100 probe coupled to a Yokogawa 7561 Digital Multimeter. The ternary systems were prepared considering aqueous solution of K<sub>3</sub>PO<sub>4</sub> (40 wt%), and aqueous solutions of the different PILs with variable concentrations (ranging from 25 to 40 wt%). Repetitive drop-wise addition of the K<sub>3</sub>PO<sub>4</sub> aqueous solution to each PIL aqueous solution was carried out until the appearance of a cloudy solution (biphasic region), followed by the drop-wise addition of ultra-pure water until the formation of a clear and limpid solution (monophasic region). All the additions occurred under constant stirring. The ternary system compositions were determined by weight quantification of all components within an uncertainty of ± 10<sup>-5</sup> g. This procedure was repeated until the acquisition of sufficient data to construct the phase diagrams.

For the determination of each tie-line (*TL*), a ternary mixture with specific concentration within the biphasic region was prepared by mixing adequate amounts of water, K<sub>3</sub>PO<sub>4</sub> and PIL. The mixture was then vigorously stirred and placed in an incubator at 25 °C (± 1 °C) for at least 24 h, until the phase equilibrium was reached. After carefully separated, the top and bottom phases were individually weighed within an uncertainty of ± 10<sup>-5</sup> g.

*TLs* were determined by a gravimetric method proposed by Merchuck *et al.*<sup>80</sup> The experimental binodal curves were correlated according to the following expression:

$$Y = A \exp[(BX^{0.5}) - (CX^3)] \quad (1)$$

where *Y* and *X*, are respectively, the PIL and the K<sub>3</sub>PO<sub>4</sub> mass fraction percentages, while *A*, *B*, and *C* are constants obtained by the regression of the experimental binodal data. The *TLs* were determined by solving the system of four equations, Eq. (2-5), and four unknown values (*Y*<sub>*T*</sub>, *Y*<sub>*B*</sub>, *X*<sub>*T*</sub> and *X*<sub>*B*</sub>):<sup>80</sup>

$$Y_T = A \exp[(BX_T^{0.5}) - (CX_T^3)] \quad (2)$$

$$Y_B = A \exp[(BX_B^{0.5}) - (CX_B^3)] \quad (3)$$

$$Y_T = \frac{Y_M}{\alpha} - \frac{1-\alpha}{\alpha} Y_B \quad (4)$$

$$X_T = \frac{X_M}{\alpha} - \frac{1-\alpha}{\alpha} X_B \quad (5)$$

where *X* and *Y* represent the weight fractions of the K<sub>3</sub>PO<sub>4</sub> and PIL, respectively; *α* is the ratio between the mass of the top phase and the total mass of the mixture; and the subscripts *T*, *B* and *M* denote the top phase, the bottom phase and the mixture, respectively.

The tie-line length (*TLL*) of each tie-line was calculated as follows:

$$TLL = \sqrt{(X_T - X_B)^2 + (Y_T - Y_B)^2} \quad (6)$$

where *X* and *Y* are the weight fraction percentages of the K<sub>3</sub>PO<sub>4</sub> and PIL, respectively; and the subscripts *T* and *B* denote the top phase and the bottom phase, respectively. Note that, the top phase is the PIL-rich phase, while the bottom phase is the K<sub>3</sub>PO<sub>4</sub>-rich phase.

### pH determination

The pH values ( $\pm 0.01$ ) of both the PIL-rich and the salt-rich phases were measured at 25 °C using a FE20/EL20 pH meter from Mettler Toledo. The pH meter was calibrated with two buffers (pH values of 4.00 and 7.00).

### Density and viscosity determination

Measurements of viscosity and density were performed at 25 °C under atmospheric pressure using an automate SVM 3000 Anton Paar rotational Stabinger viscometer-densimeter. The uncertainty for the temperature, density and viscosity is  $\pm 0.02$  K,  $\pm 0.0005$  g cm<sup>-3</sup> and  $\pm 0.35$  %, respectively. Density and viscosity measurements were carried out at selected biphasic regions for both aqueous phases. At least 3 measurements of each sample were performed to ensure accuracy and the reported results are the average values. Moreover, the standard uncertainty in density and viscosity was calculated by the ratio of the standard deviation and the average of the three replicates for each sample. The highest relative standard deviation registered for the density and dynamic viscosity measurements was  $\pm 0.01$  % and  $\pm 0.93$  %, respectively.

### Partitioning of L-tryptophan

Specific mixtures within the biphasic region were selected. For each experiment, the aqueous biphasic system was prepared by mixing the exact amount of PIL, K<sub>3</sub>PO<sub>4</sub> and aqueous solution of L-tryptophan (0.80 g·dm<sup>-3</sup>). After the complete dissolution of all the components, the mixture was allowed to settle for *circa* 24 h at 25 °C ( $\pm 1$  °C), in order to achieve a complete L-tryptophan partitioning between the two phases. Subsequent to the phase separation, the L-tryptophan of both phases was quantified using a UV-vis spectrophotometer (SHIMADZU UV-1800) at the wavelength of 278.5 nm, which corresponds to the L-tryptophan maximum absorption wavelength. The calibration curve was previously established. Possible interferences of both the K<sub>3</sub>PO<sub>4</sub> and the PIL with the analytical method were taken into account and found to be of no significance considering the dilutions used in this work.

The partition coefficients of L-tryptophan ( $K_{Trp}$ ), defined as the ratio of the concentration of L-tryptophan in the PIL- and in the K<sub>3</sub>PO<sub>4</sub>-rich phases, were calculated according to:

$$K_{Trp} = \frac{[Trp]_{PIL}}{[Trp]_{K_3PO_4}} \quad (7)$$

where [Trp]<sub>PIL</sub> and [Trp]<sub>K<sub>3</sub>PO<sub>4</sub></sub> are the concentrations of L-tryptophan in the PIL and in the K<sub>3</sub>PO<sub>4</sub>-rich phases, respectively.

The extraction efficiencies of L-tryptophan were determined according to Eq. (8), where [Trp]<sub>PIL</sub> and [Trp]<sub>K<sub>3</sub>PO<sub>4</sub></sub> are the concentrations of L-tryptophan in the PIL-rich phase and in K<sub>3</sub>PO<sub>4</sub>-rich phase, respectively, and  $m_{PIL}$  and  $m_{K_3PO_4}$  are the mass of the PIL rich-phase and the K<sub>3</sub>PO<sub>4</sub>-rich phase.

$$\%EE_{Trp} = \frac{[Trp]_{PIL} \times m_{PIL}}{[Trp]_{PIL} \times m_{PIL} + [Trp]_{K_3PO_4} \times m_{K_3PO_4}} \quad (8)$$

### Conclusions

Five new poly(ionic liquid)s comprising a pyrrolidinium polycation combined with different carboxylated counter-anions were synthesized by a straightforward environmentally-friendly procedure. The ability of hydrophilic PILs to promote phase splitting in aqueous solutions of K<sub>3</sub>PO<sub>4</sub> at 25 °C and atmospheric pressure is disclosed in this work for the first time.

The obtained results indicate that phase splitting mechanism of the studied PILs + K<sub>3</sub>PO<sub>4</sub> + H<sub>2</sub>O is similar to that of ILs, where the inorganic salt is the salting out agent and thus the most hydrophobic PIL displays a larger biphasic region. The effect of temperature on the phase behaviour of PILs + K<sub>3</sub>PO<sub>4</sub> + H<sub>2</sub>O is in agreement to what has been observed for other ABS systems containing ILs + inorganic salts, ILs + amino acids, ILs + carbohydrates, ILs + PEG and polymer + polymer, where an increase in temperature decreases the immiscibility region.

Furthermore, the results shows that PIL's  $M_w$  plays a crucial role in the hydrophobicity of the polymer, and thus on its phase splitting ability, being able to reverse the hydrophobicity order of the counter-anions. However, a large increase in the PIL's  $M_w$  has a strong impact in the viscosity of the system, which might hinder its application in separation processes. On the other hand, for the synthesized pyrrolidinium-based PILs, which have similar  $M_w$ , the carboxylated counter-anions have a large influence on the phase splitting, and play an important role in the extraction of the model biomolecule (L-tryptophan) studied.

Overall, the novel results gathered in this work demonstrates that PILs are a valuable tool not only to tune the phase splitting behaviour of ABSs, but also to improve the performance of these systems for the efficient extraction of solutes.

### Acknowledgements

Liliana C. Tomé is grateful to FCT (*Fundação para a Ciência e a Tecnologia*) for her post-doctoral research grant (SFRH/BPD/101793/2014). Mehmet Isik thanks the financial support of the European Commission through the project Renaissance-ITN 289347. Isabel M. Marrucho acknowledges FCT/MCTES (Portugal) for a contract under *Investigador FCT 2012*. This work was partially supported by FCT through the projects PTDC/QUI-QUI/121520/2010 and Research Unit GREEN-it "Bioresources for Sustainability" (UID/Multi/04551/2013).

### References

- O. Green, S. Grubjesic, S. Lee and M. A. Firestone, *Polym. Rev.*, 2009, **49**, 339-360.
- D. Mecerreyes, *Prog. Polym. Sci.*, 2011, **36**, 1629-1648.
- J. Yuan and M. Antonietti, *Polymer*, 2011, **52**, 1469-1482.
- J. Yuan, D. Mecerreyes and M. Antonietti, *Prog. Polym. Sci.*, 2013, **38**, 1009-1036.
- H. Ohno and K. Ito, *Chem. Lett.*, 1998, 751-752.

6. M. Hirao, K. Ito and H. Ohno, *Electrochim. Acta*, 2000, **45**, 1291-1294.
7. R. Marcilla, J. Alberto Blazquez, J. Rodriguez, J. A. Pomposo and D. Mecerreyes, *J. Polym. Sci. Part A: Polym.*, 2004, **42**, 208-212.
8. J. Tang, H. Tang, W. Sun, H. Plancher, M. Radosz and Y. Shen, *Chem. Commun.*, 2005, 3325-3327.
9. J. E. Bara, S. Lessmann, C. J. Gabriel, E. S. Hatakeyama, R. D. Noble and D. L. Gin, *Ind. Eng. Chem. Res.*, 2007, **46**, 5397-5404.
10. M. D. Green and T. E. Long, *Polym. Rev.*, 2009, **49**, 291-314.
11. R. Marcilla, J. A. Blazquez, R. Fernandez, H. Grande, J. A. Pomposo and D. Mecerreyes, *Macromol. Chem. Phys.*, 2005, **206**, 299-304.
12. W. Ogihara, S. Washiro, H. Nakajima and H. Ohno, *Electrochim. Acta*, 2006, **51**, 2614-2619.
13. J. Tang, H. Tang, W. Sun, M. Radosz and Y. Shen, *Polymer*, 2005, **46**, 12460-12467.
14. R. Marcilla, F. Alcaide, H. Sardon, J. A. Pomposo, C. Pozo-Gonzalo and D. Mecerreyes, *Electrochem. Commun.*, 2006, **8**, 482-488.
15. M. Hamed, L. Herlogsson, X. Crispin, R. Marcilla, M. Berggren and O. Inganäs, *Adv. Mater.*, 2009, **21**, 573-577.
16. G. B. Appetecchi, G. T. Kim, M. Montanino, M. Carewska, R. Marcilla, D. Mecerreyes and I. De Meatza, *J. Power Sources*, 2010, **195**, 3668-3675.
17. A. S. Shaplov, R. Marcilla and D. Mecerreyes, *Electrochim. Acta*, 2015, **175**, 18-34.
18. T. Fukushima, A. Kosaka, Y. Yamamoto, T. Aimiya, S. Notazawa, T. Takigawa, T. Inabe and T. Aida, *Small*, 2006, **2**, 554-560.
19. M. Antonietti, Y. Shen, T. Nakanishi, M. Manuelian, R. Campbell, L. Gwee, Y. A. Elabd, N. Tambe, R. Crombez and J. Texter, *ACS Appl. Mater. Interfaces*, 2010, **2**, 649-653.
20. T. Kim, H. Lee, J. Kim and K. S. Suh, *ACS Nano*, 2010, **4**, 1612-1618.
21. J. Yuan and M. Antonietti, *Macromolecules*, 2011, **44**, 744-750.
22. J. Tang, W. Sun, H. Tang, M. Radosz and Y. Shen, *Macromolecules*, 2005, **38**, 2037-2039.
23. A. Wilke, J. Yuan, M. Antonietti and J. Weber, *ACS Macro Lett.*, 2012, **1**, 1028-1031.
24. Y. S. Vygodskii, A. S. Shaplov, E. I. Lozinskaya, P. S. Vlasov, I. A. Malyskina, N. D. Gavrilova, P. Santhosh Kumar and M. R. Buchmeiser, *Macromolecules*, 2008, **41**, 1919-1928.
25. M. Döbbelin, R. Tena-Zaera, R. Marcilla, J. Iturri, S. Moya, J. A. Pomposo and D. Mecerreyes, *Adv. Funct. Mater.*, 2009, **19**, 3326-3333.
26. J. Yuan, C. Giordano and M. Antonietti, *Chem. Mater.*, 2010, **22**, 5003-5012.
27. J. Yuan, H. Schlaad, C. Giordano and M. Antonietti, *Eur. Polym. J.*, 2011, **47**, 772-781.
28. P. T. Nguyen, E. F. Wiesenauer, D. L. Gin and R. D. Noble, *J. membr. Sci.*, 2013, **430**, 312-320.
29. L. C. Tomé, D. Mecerreyes, C. S. R. Freire, L. P. N. Rebelo and I. M. Marrucho, *J. Mater. Chem. A*, 2014, **2**, 5631-5639.
30. Y. Ye, K. K. Stokes, F. L. Beyer and Y. A. Elabd, *J. membr. Sci.*, 2013, **443**, 93-99.
31. L. C. Tomé, A. S. L. Gouveia, C. S. R. Freire, D. Mecerreyes and I. M. Marrucho, *J. membr. Sci.*, 2015, **486**, 40-48.
32. T. D. Ho, A. J. Canestraro and J. L. Anderson, *Anal. Chim. Acta*, 2011, **695**, 18-43.
33. Y. Kohno and H. Ohno, *Aust. J. Chem.*, 2012, **65**, 91-94.
34. M. Díaz, A. Ortiz and I. Ortiz, *J. membr. Sci.*, 2014, **469**, 379-396.
35. S. T. Hemp, M. H. Allen, M. D. Green and T. E. Long, *Biomacromolecules*, 2012, **13**, 231-238.
36. M. M. Obadia, B. P. Mudraboyina, A. Serghei, T. N. T. Phan, D. Gígenes and E. Drockenmüller, *ACS Macro Lett.*, 2014, **3**, 658-662.
37. B. P. Mudraboyina, M. M. Obadia, I. Allaoua, R. Sood, A. Serghei and E. Drockenmüller, *Chem. Mater.*, 2014, **26**, 1720-1726.
38. M. Isik, R. Gracia, L. C. Kollnus, L. C. Tomé, I. M. Marrucho and D. Mecerreyes, *ACS Macro Lett.*, 2013, **2**, 975-979.
39. Y. Kohno and H. Ohno, *Chem. Commun.*, 2012, **48**, 7119-7130.
40. Y. Men, H. Schlaad and J. Yuan, *ACS Macro Lett.*, 2013, **2**, 456-459.
41. Y. Kohno, S. Saita, Y. Men, J. Yuan and H. Ohno, *Polym. Chem.*, 2015, **6**, 2163-2178.
42. A. Gandini, *Green Chem.*, 2011, **13**, 1061-1083.
43. S. A. Miller, *ACS Macro Lett.*, 2013, **2**, 550-554.
44. G. Godeau, L. Navailles, F. Nallet, X. Lin, T. J. McIntosh and M. W. Grinstaff, *Macromolecules*, 2012, **45**, 2509-2513.
45. M. Moreno, M. Ali Aboudzadeh, M. J. Barandiaran and D. Mecerreyes, *J. Polym. Sci. Part A: Polym.*, 2012, **50**, 1049-1053.
46. E. I. Privalova, E. Karjalainen, M. Nurmi, P. Mäki-Arvela, K. Eränen, H. Tenhu, D. Y. Murzin and J.-P. Mikkola, *ChemSusChem*, 2013, **6**, 1500-1509.
47. M. G. Freire, A. F. M. Claudio, J. M. M. Araujo, J. A. P. Coutinho, I. M. Marrucho, J. N. C. Lopes and L. P. N. Rebelo, *Chem. Soc. Rev.*, 2012, **41**, 4966-4995.
48. K. E. Gutowski, G. A. Broker, H. D. Willauer, J. G. Huddleston, R. P. Swatloski, J. D. Holbrey and R. D. Rogers, *J. Am. Chem. Soc.*, 2003, **125**, 6632-6633.
49. A.-L. Pont, R. Marcilla, I. De Meatza, H. Grande and D. Mecerreyes, *J. Power Sources*, 2009, **188**, 558-563.
50. V. Jovanovski, G. Cabañero, H. Grande and D. Mecerreyes, *Macromol. Symp.*, 2012, **311**, 77-82.
51. L. C. Tomé, D. Mecerreyes, C. S. R. Freire, L. P. N. Rebelo and I. M. Marrucho, *J. membr. Sci.*, 2013, **428**, 260-266.
52. L. C. Tomé, M. A. Aboudzadeh, L. P. N. Rebelo, C. S. R. Freire, D. Mecerreyes and I. M. Marrucho, *J. Mater. Chem. A*, 2013, **1**, 10403-10411.
53. L. C. Tomé, M. Isik, C. S. R. Freire, D. Mecerreyes and I. M. Marrucho, *J. membr. Sci.*, 2015, **483**, 155-165.
54. R. S. Bhavsar, S. C. Kumbharkar and U. K. Kharul, *J. membr. Sci.*, 2012, **389**, 305-315.
55. V. Jovanovski, R. Marcilla and D. Mecerreyes, *Macromol. Rapid Commun.*, 2010, **31**, 1646-1651.

56. M. Döbbelin, I. Azcune, M. Bedu, A. Ruiz de Luzuriaga, A. Genua, V. Jovanovski, G. Cabañero and I. Odriozola, *Chem. Mater.*, 2012, **24**, 1583-1590.
57. K. Fukumoto, M. Yoshizawa and H. Ohno, *J. Am. Chem. Soc.*, 2005, **127**, 2398-2399.
58. Y. Fukaya, Y. Iizuka, K. Sekikawa and H. Ohno, *Green Chem.*, 2007, **9**, 1155-1157.
59. R. D. Rogers and J. Zhang, *J. Chromatogr. B*, 1996, **680**, 231-236.
60. H. Passos, A. C. A. Sousa, M. R. Pastorinho, A. J. A. Nogueira, L. P. N. Rebelo, J. A. P. Coutinho and M. G. Freire, *Anal. Methods*, 2012, **4**, 2664-2667.
61. X. Liu, Z. Li, Y. Pei, H. Wang and J. Wang, *J. Chem. Thermodyn.*, 2013, **60**, 1-8.
62. J. F. B. Pereira, K. A. Kurnia, O. A. Cojocar, G. Gurau, L. P. N. Rebelo, R. D. Rogers, M. G. Freire and J. A. P. Coutinho, *Phys. Chem. Chem. Phys.*, 2014, **16**, 5723-5731.
63. M. G. Freire, J. F. B. Pereira, M. Francisco, H. Rodríguez, L. P. N. Rebelo, R. D. Rogers and J. A. P. Coutinho, *Chem. Eur. J.*, 2012, **18**, 1831-1839.
64. T. Mourão, L. C. Tomé, C. Florindo, L. P. N. Rebelo and I. M. Marrucho, *ACS Sustainable Chemistry & Engineering*, 2014, **2**, 2426-2434.
65. S. Shahriari, L. C. Tomé, J. M. M. Araujo, L. P. N. Rebelo, J. A. P. Coutinho, I. M. Marrucho and M. G. Freire, *RSC Adv.*, 2013, **3**, 1835-1843.
66. D. J. S. Patinha, F. Alves, L. P. N. Rebelo and I. M. Marrucho, *J. Chem. Thermodyn.*, 2013, **65**, 106-112.
67. S. P. M. Ventura, C. M. S. S. Neves, M. G. Freire, I. M. Marrucho, J. Oliveira and J. A. P. Coutinho, *J. Phys. Chem. B*, 2009, **113**, 9304-9310.
68. J. G. Huddleston, H. D. Willauer and R. D. Rogers, *J. Chem. Eng. Data*, 2003, **48**, 1230-1236.
69. A. Glyk, T. Scheper and S. Beutel, *J. Chem. Eng. Data*, 2014, **59**, 850-859.
70. Z. Du, Y.-L. Yu and J.-H. Wang, *Chem. Eur. J.*, 2007, **13**, 2130-2137.
71. Y. Chen, Y. Meng, S. Zhang, Y. Zhang, X. Liu and J. Yang, *J. Chem. Eng. Data*, 2010, **55**, 3612-3616.
72. R. M. de Oliveira, J. S. d. R. Coimbra, L. A. Minim, L. H. M. da Silva and M. P. Ferreira Fontes, *J. Chem. Eng. Data*, 2008, **53**, 895-899.
73. T. Murugesan and M. Perumalsamy, *J. Chem. Eng. Data*, 2005, **50**, 1392-1395.
74. M. T. Zafarani-Moattar, R. Sadeghi and A. A. Hamidi, *Fluid Phase Equilib.*, 2004, **219**, 149-155.
75. Y. Wang, Y. Wu, L. Ni, J. Han, J. Ma and Y. Hu, *J. Chem. Eng. Data*, 2012, **57**, 3128-3135.
76. J. F. B. Pereira, A. S. Lima, M. G. Freire and J. A. P. Coutinho, *Green Chem.*, 2010, **12**, 1661-1669.
77. M. Lu and F. Tjerneld, *J. Chromatogr. A*, 1997, **766**, 99-108.
78. A. Salabat, M. H. Abnosi and A. Motahari, *J. Chem. Eng. Data*, 2008, **53**, 2018-2021.
79. F. J. Deive, A. Rodriguez, A. B. Pereiro, J. M. M. Araujo, M. A. Longo, M. A. Z. Coelho, J. N. C. Lopes, J. M. S. S. Esperanca, L. P. N. Rebelo and I. M. Marrucho, *Green Chem.*, 2011, **13**, 390-396.
80. J. C. Merchuk, B. A. Andrews and J. A. Asenjo, *J. Chromatogr. B*, 1998, **711**, 285-293.